RESEARCH ARTICLE

For reprint orders, please contact: reprints@futuremedicine.com

Future CARDIOLOGY

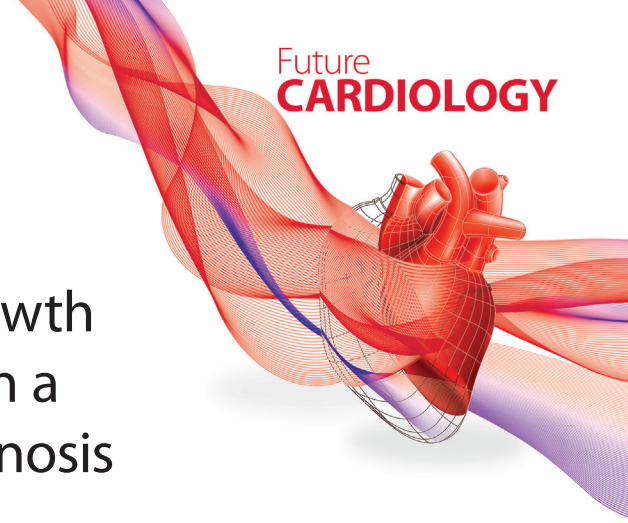

Gene expression of cytokines, growth factors and apoptosis regulators in a neonatal model of pulmonary stenosis

Peter N Liersch[1], Andreas Schwarz[1], Joerg Sachweh[2], Benita Hermanns-Sachweh[3], Ruth Heying[4], Jaime F Vázquez-Jimènez[2], Adelin Albert[5] & Marie-Christine Seghaye*[,6]

ABSTRACT **Background:** Right ventricular remodeling due to pulmonary stenosis increases morbidity in children. Its pathophysiology needs to be clarified. **Methods:** Six newborn lambs underwent pulmonary arterial banding, seven sham operation. mRNA encoding for cytokines, growth factors and regulators of apoptosis was sequentially measured in myocardium and blood before and up to 12 weeks postoperatively. **Results:** Experimental animals showed hypertrophy and fibrosis of the right ventricular myocardium, myocardial over-expression of CT-1-mRNA and higher blood concentrations of mRNA encoding for VEGF, TGF-β, Bak and BcL-xL than controls, respectively. **Conclusion:** Neonatal pulmonary stenosis leads to myocardial hypertrophy that is associated with CT-1 gene expression and with activation of growth- and apoptosis pathways in blood cells.

KEYWORDS
• apoptosis • congenital cardiac disease • cytokines • experimental model • growth factors • myocardial • myocardial hypertrophy • pulmonary stenosis • remodeling

Chronic right ventricular (RV) pressure overload in children with congenital cardiac diseases is common but its consequences in terms of remodeling of myocardial tissue have only been addressed in few studies [1,2]. Irrespective of the origin of pressure overload and of the cardiac ventricle affected, adaptive hypertrophy may evolve in a pathological state of remodeling. This state is characterized by loss of cardiomyocytes due to cell death or to phenotype transformation in myofibroblasts, initiating and entertaining myocardial fibrosis and myocardial dysfunction [3–5]. In this respect, a central role is attributed to the TGF-β. TGF-β works as a downstream effector of the renin–angiotensin system (RAS) activated by mechanical stretch. It mediates angiotensin (Ang) II-induced cardiomyocyte hypertrophy and myofibroblast synthesis of fibronectin and collagen type I and III [5].

Besides this, inflammatory pathways such as the JAK/STAT pathway are also stimulated by mechanical stretch, partly depending on AngII and mainly on the IL-6 family of cytokines to which cardiotrophin (CT)-1 belongs [6]. CT-1 is synthetized in the myocardium that it normally protects by promoting cellular proliferation and survival, among others by inducing protective heat shock proteins. However, it also promotes hypertrophy and fibrosis [7].

Loss of cardiomyocytes by apoptosis takes an important place in the mechanisms of myocardial remodeling [3]. Cardiomyocytes express members of the BCL2 family, comprising initiators, regulators and inhibitors of the intrinsic apoptotic pathway [3]. Thus, inflammation, growth and apoptosis

[1]Department of Pediatric Cardiology, University Hospital Aachen, Germany
[2]Department of Pediatric Cardiac Surgery, University Hospital Aachen, Germany
[3]Institute for Pathology, University Hospital Aachen, Germany
[4]Department of Pediatric Cardiology, University Hospital Leuven, Belgium
[5]Medical Informatics & Biostatistics, University Hospital Liège, Belgium
[6]Department of Pediatrics, University Hospital Liège, Belgium
*Author for correspondence: Tel.: +32 43679275; Fax: +32 43679475; mcseghaye@chu.ulg.ac.be

Future Medicine part of fsg

are part of a complex networking where both intensity and duration of myocardial overload are expected to influence the dynamic process of myocardial remodeling [8–12].

Previous studies have generally focused on myocardial cells as targets of hemodynamic overload and site of production of proteins involved in myocardial remodeling. However, in congenital cardiac defects generating intracardiac turbulent flow, circulating cells are submitted to sustained shear stress that could also stimulated inflammatory, growth and apoptotic signals [13].

We therefore studied the effect of pulmonary banding on blood- and myocardial cell concentrations of mRNA coding for inflammatory cytokines, growth factors and regulators of apoptosis in neonatal lambs over a time period of 12 weeks.

We show that our model of pulmonary stenosis is suitable to create myocardial hypertrophy that relates to myocardial gene expression of CT-1. In addition to that, we demonstrate that blood cells submitted *in vivo* to high shear stress are stimulated to express higher levels of mRNA coding for VEGF, TGF-β and apoptosis regulatory proteins, respectively. This expression increases over time.

Circulating blood cells might therefore be actors in the pathophysiology of myocardial remodeling consecutive to congenital cardiac defects.

Methods

Ethics statement: this study was approved by the German federal state agency supervising animal experimentations and conducted according to the guidelines of the German Animal Protection Law (Department for Animal Protection, District Government Cologne; 50.203.2 AC 40, 32/04).

Animals: 13 newborn lambs (merino mix) born at the Institute for Veterinary Medicine, University Hospital Aachen, were randomly assigned to the experimental group (n = 6) or to the control group (n = 7). Animals were cared for by the ewe pre- and post-operatively. Human medical care was ensured at each step of the experiment until euthanasia.

Anesthesia and operation: the operation was performed at the age of 3.3 ± 1.3 days (weight: 5768 ± 1114 g). Anesthesia was induced with 4% isofluran mixed with oxygen and

Table 1. Primer nucleotide sequence used for real-time PCR.

Target genes	Accession number	Base pair	Primer	Nucleotide sequence
TNF-α	X55152	199	sTNF-αTfor	CTTCAACAGGCCTCTGGTTC
			sTNF-αTrev	GATGAGGTAAAGCCCGTCAG
IL-1β	NM_001009465	200	sIL-1ß_for	CGAACATGTCTTCCGTGATG
			sIL-1ß_rev	AGAGGAGGTGGAGAGCCTTC
IL-6	NM_001009392	173	sIL-6_for	TGACATGCTGGAGAAGATGC
			sIL-6_rev	TCTGACCAGAGGAGGGAATG
IL-8	NM_001009401	203	sIL-8_for	CTGCTCTCTGCAGCTCTGTG.
			sIL-8_rev	TTGGGGTCTAAGCACACCTC
IL-10	NM_001009327	212	sIL-10_for	CGCTGTCATCGTTTTCTGCC
			sIL-10_rev	GAGTCTAGTCGAGTCACCATCC
CT-1	XM_592709	195	sCT-1_or	GCCTGGAAGAAGTGGTCAAG
			sCT-1_rev	TGCTGCACATATTCCTGGAG
VEGF	NM_001025110.1	192	sVEGF_for	CCTTGCTGCTCTACCTTCAC
			sVEGF_rev	CACAGGACGGCTTGAAAATG
TGFß1	NM_001009400	189	sTGFß1_for	ACATCAACGGGTTCAGTTCC
			sTGFß1_rev	GCTGACGAACACAGCAGTTC
FAS-L	AB011671	205	sFASag_for	ATGCCAGAATGTGTGCTCTG
			sFASag_rev	TGCAAGGGTTACAGTGTTCG
BAK	AF164518	212	sBAK_for	GCCTACTGACCCAGAGATGG
			sBAK_rev	AGTTGATGCCGCTCTCAAAC
BCL2 XL	NM_001009226	210	sBCL2lg_for	ATCGCAACTTGGATGGCTAC
			sBCL2lg_rev	TGGTCATTTCCGACTGAAGA
18S	AY753190	217	s18S_for	GGGATGCGTGCATTTATCAG
			s18S_rev	ACCCTGATTCCCCGTCAC

Table 2. Time evolution of hemodynamic variables in animals having undergone pulmonary artery banding or sham operation.

Variable	Group	1 week	4 weeks	12 weeks	p-value
P PA-RV (mmHg)	PAB	28.0 ± 12.5	42.2 ± 15.1	56.7 ± 8.4	< 0.0001
	Sham	7.7 ± 3.5	6.4 ± 2.1	5.4 ± 1.5	
RVP/SP	PAB	0.63 ± 0.10	0.75 ± 0.20	0.79 ± 0.10	< 0.0001
	Sham	0.37 ± 0.09	0.26 ± 0.05	0.25 ± 0.03	
HR (b/min)	PAB	184.2 ± 22.4	149.0 ± 29.9	114.8 ± 25.0	0.32
	Sham	191.1 ± 28.1	132.1 ± 16.2	103.1 ± 17.6	
RAP (mmHg)	PAB	4.33 ± 1.75	3.17 ± 2.96	7.80 ± 5.26	0.47
	Sham	1.43 ± 2.14	3.18 ± 2.96	3.86 ± 3.38	
SaO_2 (%)	PAB	99.3 ± 0.8	99.5 ± 0.8	98.2 ± 1.4	0.24
	Sham	96.9 ± 2.5	98.6 ± 2.3	98.4 ± 1.8	

Comparison of the response curves over the time period of 12 weeks in both groups was performed by Zerbe's test.
HR: Heart rate; P PA-RV: Systolic pulmonary arterial pressure to systolic right ventricular pressure gradient; PAB: Pulmonary artery banding; RAP: Right atrial pressure; RVP/SP: Systolic right ventricular to systolic systemic arterial pressure ratio; SaO_2: arterial oxygen saturation.

maintained with 0.8–1.5% isofluran mixed with oxygen, and fentanyl sulfate. Animals were mechanically ventilated. Arterial pressure was recorded via an arterial line put into an auricular artery.

The chest was opened in the fourth left sided intercostal space. After preparation of the great vessels and placement of a catheter in the RV via needle puncture of RV outflow tract, the pulmonary artery banding (PAB; C. R. Bard Inc., NJ, USA) was tied around the trunk of the pulmonary artery (PA) in the experimental group to achieve half of the systemic pressure proximal to the banding. The chest was closed, anesthesia stopped and animals rapidly extubated. The control group underwent sham operation with thoracotomy and preparation of the great vessels but without PAB, ensuring similar operation times to the experimental group.

Postoperative treatment consisted of intramuscular administration of flunixin and buprenorphin hydrochloride for pain management.

Cardiac catheterization (C) was performed under sterile conditions by the same investigator 1, 4 and 12 weeks after the operation (C1, C2 and C3, respectively). General anesthesia was conducted as described for the operation, apart from additional administration of propofol (1 mg/kg BW iv.). A sheet was introduced into the right jugular vein per seldinger technique. Intracardiac pressures were recorded via a Behrman Angiografic Balloon Catheter (Arrow® 4 Fr, 50 cm) in the right atrium (RA), right ventricle (RV), trunk of the pulmonary artery (PA) and right pulmonary artery (RPA) under fluoroscopy. After deflating the balloon a withdrawal curve was recorded from the RPA back to the RA, concomitantly to the record of the systemic arterial pressure, heart rate, blood gas analysis and transcutaneous oxygen saturation. After C1 and C2, lambs returned to the pen following a 30-min. period of stabilization. At C3, following hemodynamic study, a Longsheet-Introducer (Cordis® 7 Fr, 43 cm) was advanced via the right jugular vein in the RV with the tip close to the septum and a biopsy forceps (Cordis® 7 Fr, 50 cm) was introduced and five to ten biopsies were taken. At the end of the intervention, lambs were euthanized by intravenous injection of pentobarbital sodium.

The chest was then quickly opened and the the aortic valve and 1 cm above the PA bifurcation. The tissue for histological processing was obtained in a flat and a longitudinal section and preserved in formaldehyde solution (3.5%) at room temperature. The samples for electron microscopy were cut into 1–2 mm^3 cubes and placed in a solution of glutaraldehyde and phosphate buffer.

• Morphometrics

The heart was weighed and measurements of the thicknesses of the anterior wall of the RV (15 mm under the pulmonary valve annulus), the interventricular septum (10 mm under the aortic valve annulus) and the posterior wall of the left ventricle were performed (10 mm below the atrio-ventricular valve plane).

• Histology

The tissue samples were fixed in formalin and embedded in paraffin. Sections of 3 mm

Table 3. Morphometric and histological data of animals belonging to the pulmonary artery banding (n = 6) or to the sham-operated group (n = 7).

Variable	PAB	Sham	p-value
Heart/body weight ratio	0.007 ± 0.001	0.005 ± 0.001	0.0027
RV wall thickness (mm)	8.8 ± 0.7	4.29 ± 0.76	0.0023
LV wall thickness (mm)	12.2 ± 1.2	10.1 ± 0.7	0.012
IV septum thickness (mm)	11.7 ± 0.5	9.21 ± 0.4	0.0017
Cardiomyocyte diameter (µm)	18.4 ± 1.8	12.2 ± 1.5	0.0027
Cardiomyocyte nucleus diameter (µm)	5.4 ± 0.4	4.1 ± 0.2	0.0027

Right (RV) and left ventricular (LV) wall and interventricular (IV) septum were measured immediately after cardiac explantation. Comparisons between groups were performed by the Kruskal–Wallis test.
PAB: Pulmonary artery banding.

thickness were stained with hematoxylin & eosin and van-Gieson. Signs of inflammation, fibrosis, hydrops, necrosis and ischemia were recorded.

Fiber diameter and nuclear size (µm) were measured in 15 randomly selected cells in each animal by using a morphometric program (Diskus software, Carl H Hilgers, Königswinter, Germany) and the average was calculated.

• Electron microscopy

For electron microscopy, specimens were embedded in epoxy resin according to routine procedures. Semi-thin sections were stained with toluidin blue for light microscopy. Ultrathin sections were contrast enhanced with uranyl acetate and lead citrate, and examined with a Philips T400 electron microscope. Specimens were investigated with regard to hypertrophic and ischemic changes, changes in organelle structures and other signs of myocardial remodeling.

• Real-time PCR

Measurement of the expression of mRNA encoding for cytokines, growth factors and regulators of apoptosis in blood and myocardium: Before surgery and before C1, C2 and C3, 2.7 ml venous blood was collected on EDTA tubes. Qiamp RNA Blood Mini Kit (QIAGEN Hilden® Germany) was used according to the manufacturer's protocol for the isolation of RNA.

Endomyocardial biopsies were taken at C3 from the septal aspect of the RV and immediately snap frozen in liquid nitrogen until RNA isolation, that was performed with RNeasy® Micro-Kit (QIAGEN, Hilden, Germany), according to the manufacturer's recommendation. Isolated RNA from blood and myocardium was reverse transcribed to complementary DNA (cDNA) using iScriptTM cDNA Synthesis Kit (BioRad, Germany). A standard for each primer set was generated for quantitative real-time reverse transcription-PCR by cloning PCR products in pBluescript and the identity was verified by sequencing. A 2 µl cDNA sample was incubated with 20 µl QuantiTect Mix containing fluorescence dye SYBR Green (QIAGEN Hilden® Germany) and 0.6 µmol/l of each primer pair. PCR amplification was performed after initial denaturation at optimized annealing temperatures for each primer pair using MJ Research Opticon 2 (Biozym). Melting curves were acquired by stepwise increase of the temperature from 55–95°C. Threshold cycles (CTs) of real-time PCR curves were determined by Opticon® Monitor software (Biorad, CA, USA). The difference of the CTs (ΔCT) of targets and 18S-RNA housekeeping control gene reflected the amount of target mRNA in each sample. Target mRNA was quantified according to standard curve and normalized to levels of 18S-RNA. Primer sequences are shown in (Table 1).

Statistical analysis

Results were expressed as mean and SD. On graphs, means were plotted with their standard error (SE). The Kruskal–Wallis test was used to compare quantitative data in the two groups. Response curves obtained by linear interpolation between sequential time points were compared between the two groups by Zerbe's nonparametric method. This method allows not only the comparison of the two mean response curves over the entire experimental period but also over any time interval or at any time point [14]. Correlations were analyzed by the Spearman rank test. Results were considered significant at the 5% critical level ($p < 0.05$).

Results

• Hemodynamics

All animals were asymptomatic during the experimental period and did not require any treatment. The evolution of systolic RV pressure, systolic RV to systolic systemic arterial pressure ratio and systolic pressure gradient between RV and PA differed between the two groups ($p < 0.0001$), increasing over time in PAB animals while remaining stable in sham operated. In contrast, heart rate decreased similarly in both groups and SaO_2 did not change over time. The evolution of RA pressure was comparable in treated and controlled animals (Table 2).

• Morphometrics & histology

In all PAB animals, the correct position of the banding around the pulmonary arterial trunk was confirmed. Their heart/body weight ratio was higher and their RV- and LV-wall thickness were increased as compared with controls (Table 3). The diameters of cardiomyocytes and of cardiomyocyte nuclei were significantly larger ($p = 0.0027$) in PAB- than in sham-operated animals (Table 3), (Figures 1 & 2). In the histological analysis, swelling of the cardiomyocytes as a sign of reversible state of imminent cell death and isolated areas of fibrosis were found in three (50%) out of six PAB animals and in none (0%) of the sham-operated (Figure 3).

• Electron microscopy

Four of the six PAB animals (67%) revealed a widening of the Z-striation (Figures 4 & 5). Actin and myosin filaments, sarcomere, mitochondria and organelle structure were intact. There was no anomaly found in the sham-operated animals.

Myocardial expression of mRNA encoding for cytokines, growth factors and markers of apoptosis: Cytokine-mRNA levels measured in the myocardium 12 weeks after surgery were similar in both groups, while CT-1 mRNA levels were significantly higher in PAB animals than in controls ($p = 0.034$). On average, levels of mRNA encoding for VEGF, TGF-β, Fas, Bak and Bcl-xL were comparable in both groups (Table 4).

In all animals, myocardial expression of CT-1 correlated with RV-PA pressure gradient measured at C3, with RV wall thickness and with cardiomyocyte and cardiomyocyte nuclei diameter (Spearman coefficient: 0.71, 0.66, 0.60 and 0.63, respectively; $p < 0.05$).

Blood cell expression of mRNA encoding for cytokines, growth factors and markers of apoptosis: Blood levels of IL-1-mRNA markedly increased in both groups during the first week after surgery, then continued to slightly increase in the PAB group and stalled in the control group. Zerbe's test however did not evidence any difference between treated and control animals ($p = 0.15$) (Figure 6). The same observations applied for the time evolution of TNF-α, IL-6, IL-8 and IL-10 blood levels, respectively (data not shown).

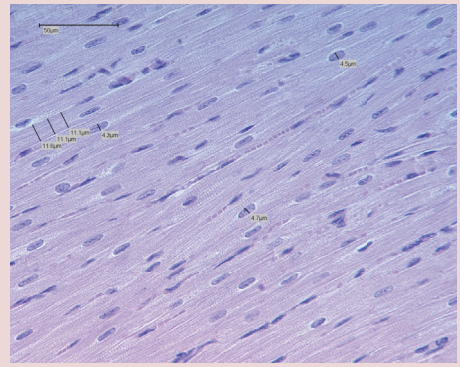

Figure 1. Representative histological study of the right ventricular myocardium of one animal having undergone sham operation showing diameter of cardiomyocytes and of nuclei. Magnification: 40×.

CT-1-mRNA blood levels could not be detected in any of the animals

VEGF-mRNA levels slightly increased over the 12-week period in PAB animals unlike in the sham group but overall the two evolution curves

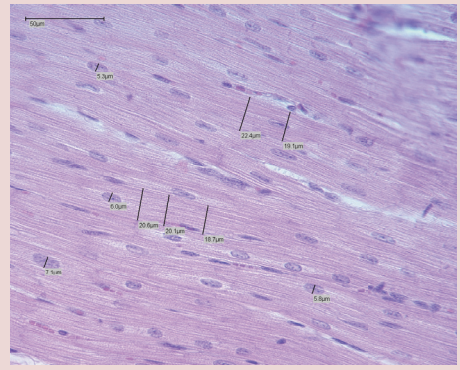

Figure 2. Representative histological study of the right ventricular myocardium of one animal having undergone pulmonary arterial banding showing diameter of cardiomyocytes and of nuclei. Magnification: 40×.

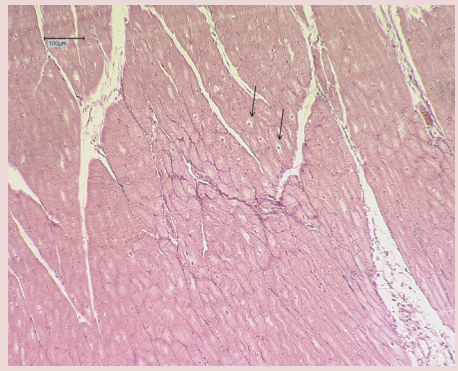

Figure 3. Representative histological study of the right ventricular myocardium of one animal having undergone pulmonary arterial banding. Arrows mark perinuclear swelling of cardiomyocytes. Areas of fibrosis are stained in red. Van Gieson stain. Magnification: 10×.

were comparable (p = 0.26) (Figure 6). However, mean blood levels of VEGF-mRNA were higher in PAB animals than in sham operated 12 weeks after surgery (p = 0.032). Considering all animals, VEGF-mRNA levels and systolic RV pressure at 12 weeks correlated with each others (Spearman coefficient: 0.72; p < 0.01).

A similar kinetics was observed for TGF-β-mRNA. Blood levels increased in both groups during the first week after surgery and thereafter continued to rise only in the PAB group. At 12 weeks, they were significantly higher than in controls (p = 0.048) but overall Zerbe's

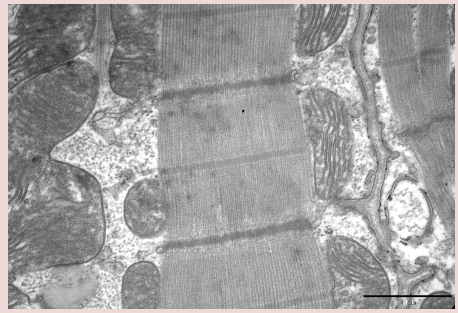

Figure 4. Representative ultrastructural study of the right ventricular myocardium of one animal having undergone sham operation. Ultrastructures shown are myofibrils with normal Z-striation, normal mitochondrion and normal sarcoplasmic reticulum. Magnification bar represents 1 μm.

showed no difference between the two evolution curves (p = 0.076) (Figure 6). In all animals, TGF-β-mRNA levels and systolic RV pressure at 12 weeks correlated with each others (Spearman coefficient: 0.67; p < 0.05).

No change in blood levels of Fas-mRNA was observed over time in the two groups (Figure 7). By contrast, levels of BcL-xL-mRNA increased continuously over the 3-month period in PAB animals compared with controls (p = 0.026) (Figure 7) and were also significantly higher at 12 weeks (p = 0.03). The evolution of Bak-mRNA paralleled that of BcL-xL but the two groups were not different (p = 0.13), although observed levels at 12 weeks post-operatively were higher in PAB animals (p = 0.049) (Figure 7). In all animals, Bak- and BcL-xL-mRNA levels and systolic RV-pressure at 12 weeks correlated with each other, respectively.

Discussion

In this study, we utilized a chronic model of pulmonary stenosis in that pressure overload was established by PAB in neonatal lambs. This model permitted to follow the animals for a period of 3 months. Indeed, most previous studies dealt with acute and short lasting pressure overload [12] or with chronic alterations due to combined pressure and volume overload of the RV in older animals [15]. We simulated hemodynamic conditions that occur commonly in congenital heart diseases, such as those associated with moderate pulmonary stenosis.

Hemodynamics and morphometrics: we observed a steady increase of RV pressure in the PAB group that reached nearly 80% of the systemic pressure after 12 weeks, associated with RV hypertrophy. The increased muscle fiber diameter in PAB lambs and the broadening of the Z-striation illustrate that RV myocardial cells depicted compensatory hypertrophy. We also observed a significant influence of RV pressure overload on the left ventricle, which also showed a significant hypertrophy of the septum and of the posterior wall. Stiffening and impaired diastolic function of the left ventricle after chronic RV overload have been reported [16,17] and systemic neuro-endocrine activation suggested to be involved in that phenomenon [16]. Whether the same mechanisms have participated to RV- and LV-hypertrophy observed in our series remains speculative.

Systemic and myocardial expression of pro- and anti-inflammatory cytokines: The

implication of inflammatory mechanisms in diseases with deterioration of cardiac pump function such as heart failure, myocardial ischemia and reperfusion or in myocardial dysfunction after cardiac surgery is widely accepted [18–20]. Activated inflammatory pathways such as the NF-κB pathway [21] also participate in adaptive mechanisms to mechanical stretch. In our study, however, circulating and myocardial levels of inflammatory cytokines with the exception of CT-1 and TGF-α were not affected by PAB in the time period of 3 months. This stays in contrast to our previous clinical study in infants in whom pro-inflammatory cytokine expression was related to the degree of RV pressure overload. In contrast to the lambs studies here, infants had heart failure due to left-to-right shunt or hypoxemia, that both might have enhance myocardial cytokine expression [22,23].

Systemic and myocardial expression of growth factors: CT-1 is a cytokine of the IL-6 family of cytokines that plays a central role in protection of neonatal and adult myocardial cells against hypoxemia or ischemia-reperfusion injury, mainly by enhancing expression of protective heat shock proteins (HSP)-70 and HSP-90 [7]. CT-1 is also involved in pathological processes of myocardial remodeling since it is a main inducer of myocardial cell hypertrophy. Indeed, gp130 knock-out animals are not able to generate a compensatory hypertrophy but show massive apoptosis in response to pressure overload, in contrast to wild type animals [24]. CT-1 stimulates collagen synthesis in myofibroblasts, thus contributing to the process of fibrosis [7]. In a recent study, we reported myocardial expression of CT-1 in infants with congenital cardiac defects with pressure overload of the RV. CT-1 expression was enhanced by hypoxemia and was associated with the activation of the Jak/STAT pathway, suggesting its implication in myocardial hypertrophy in congenital cardiac diseases [2]. Our current results showing higher myocardial CT-1-mRNA after 12 weeks in PAB than in sham operated animals support this role of CT-1.

As an interesting finding of our study, VEGF-mRNA levels were not increased in the

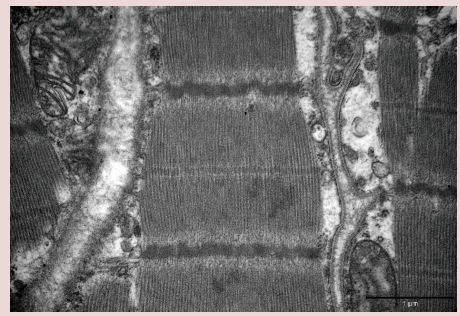

Figure 5. Representative ultrastructural study of the right ventricular myocardium of one animal having undergone pulmonary arterial banding showing widening of Z-striation. Sarcoplasmic reticulum is not enlarged, the number of ribosomes is not increased. Magnification bar represents 1 μm.

Table 4. Myocardial expression of mRNA encoding for the cytokines TNF-α, IL-1β, -6, -8, -10, for the growth factors cardiotrophin-1, VEGF, TGF-β and the regulators of apoptosis Fas, BcL-xL, and Bak in animals having undergone pulmonary artery banding (PAB; n = 6) or sham operation (n = 7).

Variable	PAB group	Sham group	p-value
TNF-α	4.88 ± 0.42	4.57 ± 0.43	0.37
IL-1β	4.92 ± 0.42	4.83 ± 0.57	0.46
IL-6	5.14 ± 0.35	5.00 ± 0.41	0.81
IL-8	5.07 ± 0.88	4.82 ± 0.69	0.42
IL-10	4.88 ± 0.25	4.76 ± 0.50	0.81
CT-1	5.03 ± 0.61	4.41 ± 0.25	0.034
VEGF	3.52 ± 0.17	3.30 ± 0.25	0.14
TGF-β	3.78 ± 0.24	3.55 ± 0.21	0.12
Fas	4.29 ± 0.32	4.07 ± 0.36	0.29
BcL-xL	3.69 ± 0.36	3.60 ± 0.31	0.68
Bak	4.71 ± 0.39	4.46 ± 0.34	0.46

The values were normalized for expression of 18S-mRNA and are shown by the mean ± standard deviation. Comparisons between groups were analyzed by the Kruskal–Wallis test.

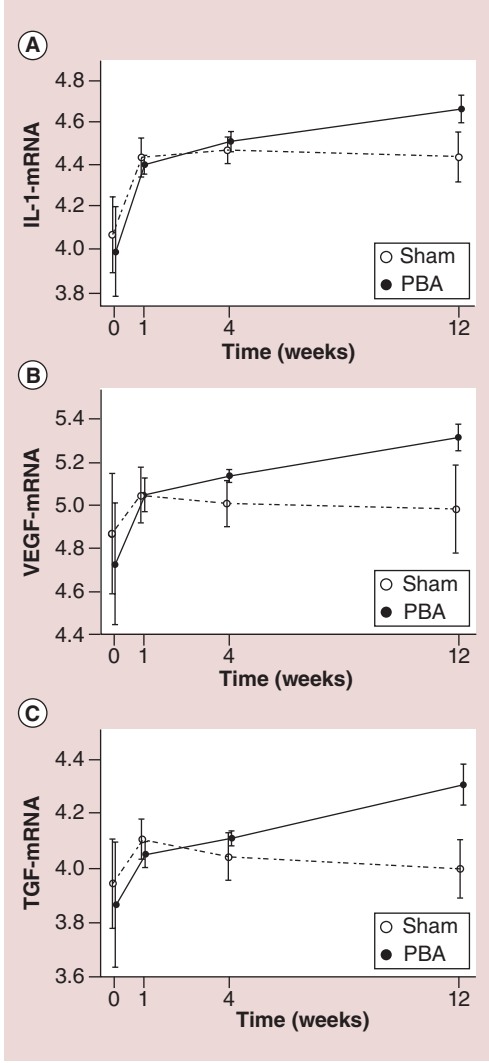

Figure 6. Time evolution of blood concentrations of mRNA encoding for Interleukin-1β, VEGF and TGF-β in animals having undergone pulmonary artery banding or sham operation. Comparison of the response curves over the time period of 12 weeks in both groups was performed by Zerbe's test and comparison of mean values at different time points by Kruskall–Wallis test. Response curves were not significantly different in both groups whereas comparison of mean values showed significantly higher VEGF- and TGF-β. mRNA 12 weeks after the operation in PAB- than in sham operated animals.
PAB: Pulmonary artery banding.

myocardium but in the circulating cells of PAB animals at the end of the study period. Platelets express VEGF-mRNA and have been suggested to be the main contributors of VEGF serum levels [25], while neutrophils and monocytes express VEGF-mRNA under inflammatory stimulation [26]. Going along with this, blood but not myocardial levels of TGF-β-mRNA were increased 3 months after the operation in PAB animals in contrast to the sham operated. This is consistent with previous report on adults with aortic stenosis and in mice with transverse aortic arch banding, where circulating and not myocardial TGF-β levels correlated with the importance of stenosis and with the LV mass index [27]. Leukocytes, endothelial cells and platelets are sources of TGF-β [13,28–29]. In this respect, a recent study has demonstrated that platelet derived TGF-β is related to LV hypertrophy, LV fibrosis and LV systolic dysfunction in a mice model of aortic stenosis [13]. Platelets contain high amounts of TGF-β and secrete it in a latent form that becomes activated by shear stress [29].

Besides its effects on the fibrotic program, TGF-β also possesses anti-inflammatory properties with deactivation of macrophages [30] that might have inhibited cytokine production in blood and myocardium of the animals studied in our series.

Systemic and myocardial expression of markers of apoptosis: apoptosis as a form of ubiquitous programmed cell death is a process that is absent in normal adult heart [3]. It never has been studied in congenital cardiac defects. In our series, chronic RV-overload did not have any effect of the expression of apoptotic regulatory proteins in the myocardium in the time period studied. This stays in contrast to a previous study that reported that acute RV overload with persistent RV failure after a transient 90 min long period of PAB induces early activation of apoptotic pathway associated to overexpression of TNF-α in dogs [13]. This discrepancy between both observations points out the importance of the intensity and duration of myocardial overload with regard to the activation of the apoptotic pathways. In our study, however, PAB animals showed higher circulating blood mRNA levels of the pro-apoptotic factor Bak and of the anti-apoptotic BcL-xL than sham operated animals. Bak and BcL-xL are both members of the BCL2 family that regulates the intrinsic apoptotic pathway. Apoptosis has been described in leukocytes and in platelets stimulated by shear stress [31,32], making these cells likely to be the site of over-expression of apoptosis regulatory proteins in our animals with PAB. Whether

apoptotic signals can be transmitted with time from circulating cells to cardiomyocytes is not known yet and must be clarified.

Conclusion

In this study, newborn lambs with moderate pulmonary stenosis developed chronic pressure overload of the RV and hypertrophy of both the right and the left ventricles. They showed continuously increasing blood – but not myocardial levels of mRNA encoding for VEGF, TGF-β, BaK and BcL-xL over a time period of 3 months. Three months after surgery, they also evidenced higher myocardial expression of mRNA encoding for CT-1 that correlated with ventricular hypertrophy.

These findings suggest that in our model, besides myocardial cells, circulating blood cells are potential early extra-cardiac source of factors involved in the pathophysiology of myocardial remodeling. While the primum movens of circulating cell activation is likely to be related to the turbulent flow in the pulmonary trunk, myocardial remodeling might entertain this activation. Blood cell-myocardial cell interactions have therefore to be clarified in further studies.

Limitation section

The assessment of a relative small set of genes at mRNA- but not at protein level in myocardium and blood cells is the main limitation of our study. Indeed, our results allow describing an association between myocardial CT-1-mRNA expression and hallmarks of compensatory hypertrophy but not demonstrating any causality between CT-1 expression and myocardial remodeling. The definitive demonstration of this causality would necessitate the inhibition of CT-1 in a third experimental group of animals. However, to the best of our knowledge, this has not been performed that far in a large animal model that has the advantage to permit some extrapolation to human pathophysiology.

Furthermore, the isolation of leucocytes and platelets and their examination with regard to the expression of growth factors would have significantly added to the comprehension of the systemic response to intracardiac turbulent flow and must be addressed in further studies.

Future perspective

Our data give evidence of the necessity to better understand the cross talk between circulating

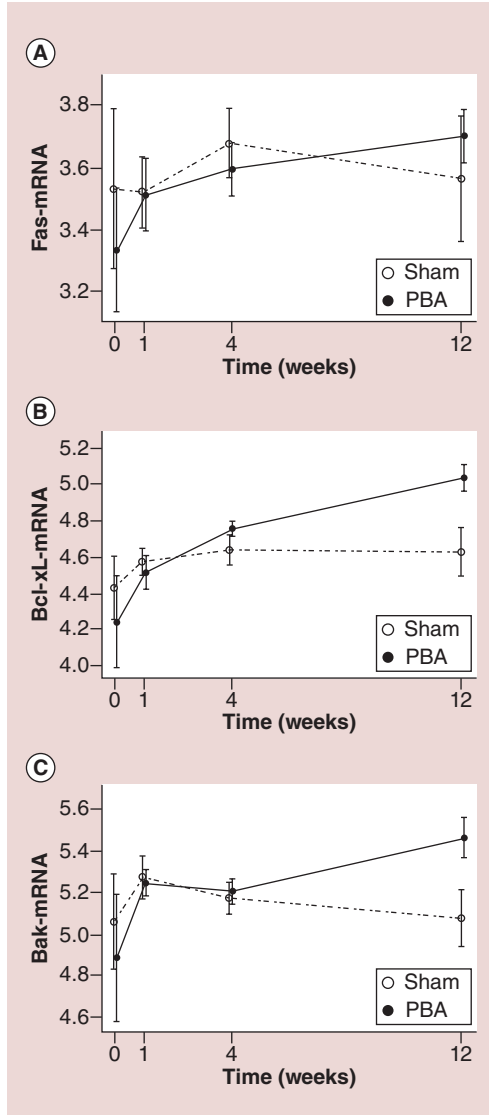

Figure 7. Time evolution of blood concentrations of mRNA encoding for the apoptosis regulating proteins Fas, BcL-xL and Bak in animals having undergone pulmonary artery banding or sham operation. Comparison of the response curves over the time period of 12 weeks in both groups was performed by Zerbe's test and comparison of mean values at different time points by Kruskall-Wallis test. Response curve and comparison of mean values were not different between groups for Fas-mRNA levels. By contrast, response curve of BcL-xL-mRNA but not of Bak-mRNA was significantly different between groups. Comparison of mean values showed significantly higher BcL-xL-mRNA and Bak-mRNA 12 weeks after the operation in PAB- than in sham operated animals.
PAB: Pulmonary artery banding.

and myocardial cells in patients with cardiac diseases in general and with congenital cardiac defects in particular. Indeed, this cross-talk might be an important part of the mechanisms leading to remodeling processes in and also outside the myocardium.

Differential gene expression in circulating blood cells might become a tool for the diagnosis and the follow up of patients with adaptive myocardial hypertrophy who are at risk to develop maladaptive remodeling with myocardial fibrosis.

Financial & competing interests disclosure

This study was supported by a grant of the Deutsche Forschungsgemeinschaft (SE 912/3–2) to MC Seghaye. The authors have no other relevant affiliations or financial involvement with any organization or entity with a financial interest in or financial conflict with the subject matter or materials discussed in the manuscript apart from those disclosed.

No writing assistance was utilized in the production of this manuscript.

Ethical conduct

The authors state that they have obtained appropriate institutional review board approval or have followed the principles outlined in the Declaration of Helsinki for all human or animal experimental investigations. In addition, for investigations involving human subjects, informed consent has been obtained from the participants involved.

EXECUTIVE SUMMARY

- Myocardial remodeling in children with congenital cardiac disease impairs survival and underlies complex mechanisms that are not well understood.
- Neonatal pulmonary stenosis induces hypertrophy of the right ventricular myocardium that is associated with gene expression of cardiotrophin-1.
- Neonatal pulmonary stenosis is associated to the activation of growth and apoptosis pathways in blood cells.

References

Papers of special note are highlighted as:
• of interest; •• of considerable interest

1 Qing M, Schumacher K, Heise K *et al.* Myocardial synthesis of pro- and anti-inflammatory cytokines in infants with congenital cardiac defects. *J. Am. Coll. Cardiol.* 41, 2266–2274 (2003).

2 Heying R, Qing M, Schumacher K et al. Myocardial cardiotrophin-1 is differentially induced in congenital cardiac defects depending on hypoxemia. *Future Cardiol.* 10, 53–62 (2014).

• **Describes the role of hypoxemia on expression of cardiotrophin-1 in infant myocardium.**

3 Dorn GW 2nd. Apoptotic and non-apoptotic programmed cardiomyocyte death in ventricular remodelling. *Cardiovasc. Res.* 81, 465–473 (2009).

4 Gustafsson AB, Gottlieb RA. Recycle or die: the role of autophagy in cardioprotection. *J. Mol. Cell. Cardiol.* 44, 654–661 (2008).

• **Describe the mechanisms of myocardial cell death in myocardial remodeling.**

5 Weber KT, Sun Y, Bhattacharya SK *et al.* Myofibroblast-mediated mechanisms of pathological remodelling of the heart. *Nat. Rev. Cardiol.* 10, 15–26 (2013).

•• **Describe the role of phenotype transformation of cardiomyocytes in myofibroblasts in myocardial remodeling.**

6 Pan J, Fukuda K, Saito M *et al.* Mechanical stretch activates the JAK/STAT pathway in rat cardiomyocytes. *Circ. Res.* 84, 1127–1136 (1999).

7 Calabrò P, Limongelli G, Riegler L *et al.* Novel insights into the role of cardiotrophin-1 in cardiovascular diseases. *J. Mol. Cell. Cardiol.* 46, 142–148 (2009).

8 Lee SH, Wolf PL, Escudero R *et al.* Early expression of angiogenesis factors in acute myocardial ischemia and infarction. *N. Engl. J. Med.* 343, 148–149 (2000).

9 Takimoto Y, Aoyama T, Iwanaga Y *et al.* Increased expression of cardiotrophin-1 during ventricular remodeling in hypertensive rats. *Am. J. Physiol. Heart Circ. Physiol.* 282, 896–901 (2002).

10 Condorelli G, Morisco C, Stassi G *et al.* Increased cardiomyocyte apoptosis and changes in proapoptotic and antiapoptotic genes bax and bcl-2 during left ventricular adaptations to chronic pressure overload in the rat. *Circulation* 99, 3071–3078 (1999).

11 Rosenkranz S. TGF-beta1 and angiotensin networking in cardiac remodeling. *Cardiovasc. Res.* 63, 423–432 (2004).

12 Dewachter C, Dewachter L, Rondelet B *et al.* Activation of apoptotic pathways in experimental acute afterload-induced right ventricular failure. *Crit. Care Med.* 38, 1405–1413 (2010).

13 Meyer A, Wang W, Qu J *et al.* Platelet TGF-β1 contributions to plasma TGF-β1, cardiac fibrosis, and systolic dysfunction in a mouse model of pressure overload. *Blood* 119, 1064–1074 (2012).

•• **Describe the role of TGF-β1 secreted by activated platelets on myocardial remodeling and fibrosis related to aortic stenosis.**

14 Zerbe GO. Randomization analysis of the completely randomized design extended to growth and response curves. *J. Am. Stat. Assoc.* 74, 215–221 (1979).

15 Lambert V, Capderou A, Le Bret E *et al.* Right ventricular failure secondary to chronic overload in congenital heart disease: an experimental model for therapeutic innovation. *J. Thorac. Cardiovasc. Surg.* 139, 1197–1204 (2010).

16 Leeuwenburgh BP, Helbing WA, Steendijk P *et al.* Biventricular systolic function in young lambs subject to chronic systemic

right ventricular pressure overload. *Am. J. Physiol. Heart Circ. Physiol.* 281, 2697–2704 (2001).

17 Leeuwenburgh BP, Helbing WA, Wenink ACG *et al.* Chronic right ventricular pressure overload results in a hyperplasic rather than a hypertrophic myocardial response. *J. Anat.* 212, 286–294 (2008).

18 Fearon WF, Fearon DT. Inflammation and cardiovascular disease: role of the interleukin-1 receptor antagonist. *Circulation* 117, 2577–2579 (2008).

19 Hövels-Gürich HH, Vazquez-Jimenez JF, Silvestri A *et al.* Production of proinflammatory cytokines and myocardial dysfunction after arterial switch operation in neonates with transposition of the great arteries. *J. Thorac. Cardiovasc. Surg.* 124, 811–820 (2002).

20 Swynghedauw B. Molecular mechanism of myocardial remodeling. *Physiol. Rev.* 79, 215–262 (1999).

21 Gordon JW, Shaw JA, Kirshenbaum LA. Multiple facets of NF-κB in the heart: to be or not to NF-κB. *Circ. Res.* 108(9), 1122–1132 (2011).

- **Review the role of the inflammatory pathway of NF-κB on myocardial hypertrophy, failure, and protection.**

22 Pulkki KJ. Cytokines and cardiomyocyte death. *Ann. Med.* 29, 339–343 (1997).

23 Qing M, Görlach A, Schumacher K *et al.* The hypoxia-inducible factor HIF-1 promotes myocardial expression of VEGF in infants with congenital cardiac defects. *Basic Res. Cardiol.* 102, 224–232 (2007).

24 Hirota H, Chen J, Betz UA *et al.* Loss of gp130 cardiac muscle cell survival pathway is a critical event in the onset of heart failure during biomechanical stress. *Cell* 97, 189–198 (1999).

25 Salgado R, Benoy I, Bogers J *et al.* Platelets and vascular endothelial growth factor (VEGF): a morphological and functional study. *Angiogenesis* 4, 37–43 (2001).

26 Hamamichi Y, Ichida F, Yu X *et al.* Neutrophils and mononuclear cells express vascular endothelial growth factor in acute Kawasaki disease: its possible role in progression of coronary artery lesions. *Pediatr. Res.* 49, 74–80 (2001).

27 Villar AV, Cobo M, Llano M *et al.* Plasma levels of transforming growth factor-beta1 reflect left ventricular remodeling in aortic stenosis. *PLoS ONE* 4, e8476 (2009).

28 Kuruvilla L, Nair RR, Umashankar PR *et al.* Endocardial endothelial cells stimulate proliferation and collagen synthesis of cardiac fibroblasts. *Cell Biochem. Biophys.* 47, 65–72 (2007).

29 Ahamed J, Burg N, Yoshinaga K *et al. In vitro* and *in vivo* evidence for shear-induced activation of latent transforming growth factor-beta1. *Blood* 112, 3650–3660 (2008).

30 Kapur NK. Transforming growth factor-β: governing the transition from inflammation to fibrosis in heart failure with preserved left ventricular function. *Circ. Heart Fail.* 4, 5–7 (2011).

31 Shive MS, Salloum ML, Anderson JM. Shear stress-induced apoptosis of adherent neutrophils: a mechanism for persistence of cardiovascular device infections. *Proc. Natl Acad. Sci. USA* 97, 6710–6715 (2000).

32 Vasina EM, Cauwenberghs S, Feijge MA *et al.* Microparticles from apoptotic platelets promote resident macrophage differentiation. *Cell Death Dis.* 2, e211 (2011).